Compact Co-Polarized PIFAs for Full-Duplex Application Based on CM/DM Cancellation Theory

Jiadong Hu, Weiquan Zhang, Yue Li, *Senior Member, IEEE*, and Zhijun Zhang, *Fellow, IEEE*

***Abstract*— In this article, a compact co-polarized decoupled antenna for full-duplex application working at 1.71 GHz is proposed. The antenna is composed of two back-to-back air-dielectric planar inverted-F antennas (PIFAs) with zero edge-to-edge distance. The whole system is included in a compact volume of $0.45\lambda_0 \times 0.45\lambda_0 \times 0.02\lambda_0$. The proposed antenna is designed based on the common mode (CM)/differential mode (DM) cancellation theory and its design guideline is illustrated in detail. Isolation maximum of 42 dB, broadside gain of 6.7 dB, and efficiency of 90% have been achieved in the proposed structure. There is a 1.9 dB gain difference between the broadside gain and the maximum gain. The proposed antenna shows its potentials in the radio frequency front-end incorporate design.**

***Index Terms*— Co-polarized decoupling, full-duplex, mode cancellation, planar inverted-F antenna (PIFA), radio frequency front-end (RFFE) incorporate design.**

I. Introduction

With the development of modern communication system, higher requirements are raised for the radio frequency front-end (RFFE), such as integrated, militarized, and lightweight. Therefore, the incorporate design of RFFE between the antenna and the transceiver is becoming a new trend and has drawn the attention of many researchers. The incorporate design of RFFE can effectively reduce the volume and weight of the communication system. What is more, the spectrum efficiency of the system can be greatly enhanced. In fact, integrating the antenna with the duplexer is the key of the RFFE incorporate design, which is the so-called full-duplex antenna.

Self-interference is the main problem that the full-duplex system needs to solve. In general, the isolation between transmitter (TX) and receiver (RX) should be higher than 100 dB, if the full-duplex system wants the same signal-to-noise ratio level as the half duplex system. The isolation of full-duplex system is devoted jointly by the antenna, the analog, and the digital cancellation parts. Therefore, isolation enhancement at the antenna part can alleviate the design difficulty of the subsequent self-interference cancellation period.

Several techniques have been proposed to enhance the isolation between the transmit and receive antennas. The polarization diversity [1]–[6] method can realize high isolation concisely. However, it needs to occupy two polarized channels, easily interfered in actual communication environment. The pattern diversity [7] creates a relative large difference of patterns between TX and RX antennas, increasing the whole system complexity. Multiple groups of TX and RX antennas are utilized to cancel out the mutual interference based on orthogonal mode [8]–[15], realizing high port isolation in wideband. Anyway, the whole system takes up much space for additional TX and RX antennas. Similarly, the complex feeding network in near-field cancellation [16]–[18] method also occupies a large area. Making use of resonators [19]–[22], circulators [23], electromagnetic bandgap (EBG) structures [24]–[27], metal walls [28], and metastructures [29], [30] can realize high isolation between one pair of TX and RX antennas, but they still need to stay a distance from each other or have a high profile. The defected ground structure (DGS) [31]–[34] can also reduce the distance between the TX and RX antennas, while the back radiation is difficult to suppress. Moreover, hybrid methods [35]–[37] are utilized to realize dual-polarized decoupling and further improve the decoupling bandwidth. Recently, the common mode (CM) and differential mode (DM) cancellation theory has been proposed and offers a new decoupling perspective [38]–[40]. Resulting from insufficient structure variables, the work of [38] and [39] cannot achieve high isolation. In [40], the CM/DM design was successfully applied in the decoupling design of mobile phone antenna. Due to the complex application occasion, the radiation pattern was difficult to control and 24 dB of in-band isolation was achieved.

In this article, a compact co-polarized antenna for full-duplex application with high port isolation is designed based on the CM/DM cancellation. The system consists of two symmetrical air dielectric planar inverted-F antennas (PIFAs), integrated into a space of $0.45\lambda_0 \times 0.45\lambda_0 \times 0.02\lambda_0$. The two PIFAs are placed with a $0.25\lambda_0$ center-to-center distance and zero edge-to-edge distance. The proposed antenna achieves the isolation of 42 dB at 1.71 GHz. There is a 1.9 dB gain difference between broadside and the maximum gain

Manuscript received September 12, 2020; revised November 14, 2020; accepted December 20, 2020. Date of publication February 24, 2021; date of current version October 28, 2021. This work was supported in part by the National Natural Science Foundation of China under Contract 61525104 and Contract 61971254, and in part by the National Key Research and Development Program of China under Grant 2018YFB1801603. *(Corresponding author: Zhijun Zhang.)*

The authors are with the Beijing National Research Center for Information Science and Technology, Tsinghua University, Beijing 100084, China (e-mail: zjzh@tsinghua.edu.cn).

Color versions of one or more figures in this article are available at https://doi.org/10.1109/TAP.2021.3060067.

Digital Object Identifier 10.1109/TAP.2021.3060067

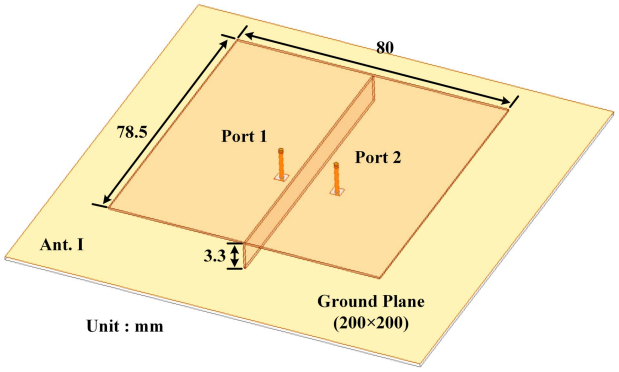

Fig. 1. Antenna I: two back-to-back air-dielectric standard PIFAs (nonproportional diagram).

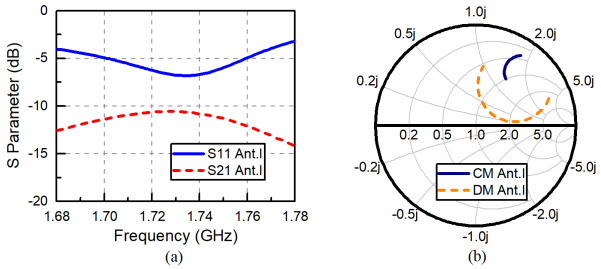

Fig. 2. Simulated results of antenna I. (a) S-parameters. (b) CM and DM impedance smith chart.

direction. The rest of this article is organized as follows. The proposed antenna schematic is presented in Section II. In Section III, the antenna mechanism and design principles are illustrated. The simulation and measurement results are provided in Section IV. Conclusions are finally drawn in Section V.

II. Antenna Mechanism and Design Principle

A. CM and DM Cancellation Theory

The CM and DM usually refer to the excitation states of a two-port network from the basic microwave theory [41]. In a symmetrical, reciprocal two-port network represented by its S-parameters (S_{ij}), the reflection coefficient of CM (S_{cc11}) and DM (S_{dd11}) satisfies the relationship [43]

$$S_{cc11} = S_{11} + S_{21}$$
$$S_{dd11} = S_{11} - S_{21}.$$

In a complete isolation network, the transmission coefficient S_{21} equals to zero, implying that $S_{cc11} = S_{dd11}$.

Two back-to-back standard PIFAs with a shared short-circuit wall are shown in Fig. 1, set as the initial model (antenna I). It is not completely matched and has an isolation of around 10 dB, as shown in Fig. 2(a). Impedance curves of both the CM and DM are shown in Fig. 2(b). They are separated from each other.

The decoupling condition that $S_{cc11} = S_{dd11}$ can also be inferred from the point of fields. The CM is excited by in-phase input, while the DM state needs out-of-phase input, as shown in Fig. 3. It can be observed that the magnitude of CM current at feeding ports is different from the DMs. Based

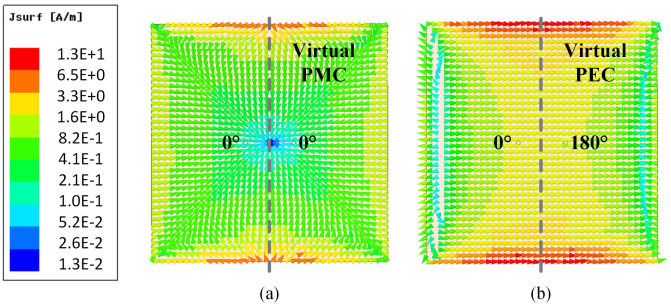

Fig. 3. Simulated current distribution of CM and DM in proposed antenna at 1.73 GHz (decoupled state). (a) CM excitation. (b) DM excitation.

on the superposition theorem, the current at port 2 will not be completely canceled if only port 1 is excited in this case, meaning that coupling between two ports. Therefore, in order to achieve high port isolation, reasonable approaches should be explored to make S_{cc11} equal to S_{dd11} for sufficient current cancellation between CM and DM.

B. Design Principle

From basic microwave theory, the network Z-parameters have the correspondence with its S-parameters. According to the analysis above, an approach is needed to make the CM impedance close to its DM impedance for decoupling. However, in practical antenna design, the impedance matching should also be accomplished. To this end, another approach is needed to match the decoupling range. Therefore, in ideal state, two approaches had better be found to tune the CM and DM impedances respectively.

C. Design Guideline

Antennas II–IV shown in Table I are the design evolution of the proposed antenna for full-duplex application. In symmetrical structures, virtual boundary conditions can be established, as shown in Fig. 3, which also exist in antennas II∼IV. The virtual PMC and PEC boundary conditions help analyze the effects of different approaches.

In antenna I, the CM impedance curve is very far from the matching point, adverse for the subsequent design. For the purpose of realizing high isolation and good matching based on antenna I, three design approaches have been proposed as follows.

1) Etch an "H"-shaped slot on the upper copper board (antenna II). This step has an effect on both CM and DM impedance, as shown in Fig. 4. Compared with antenna I, the CM impedance curve gets closer to the matching point, while the DM one is on the contrary. It is noted that the width of the middle gap of "H"-shaped slot *Ws* only affects the DM impedance. The reason is that *Ws* mainly determines the *E*-field strength excited across the gap. The virtual PEC boundary of DM supports this normal *E*-field component, while the PMC in CM does not.
2) Add a metal strip to connect two inner conductors (antenna III). The metal strip and the straight slot constitute a length of CPW transmission line. The introduction

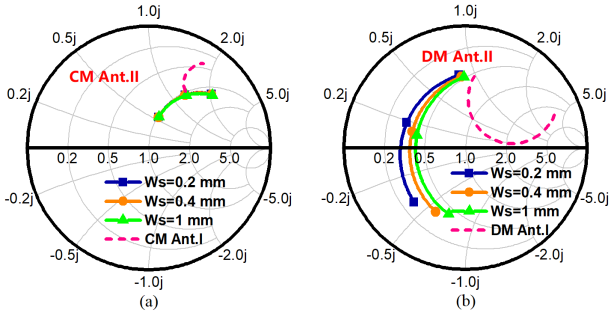

Fig. 4. Impedance smith charts of Antenna II with varying Ws. (a) CM. (b) DM.

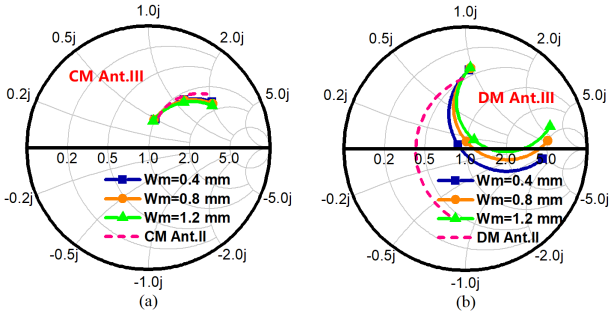

Fig. 5. Impedance smith charts of Antenna III with varying Wm. (a) CM. (b) DM.

of the metal strip makes the DM impedance curve back to the nearby of matching point, but has little effect on the CM impedance. The CPW line becomes open-ended when the virtual PMC of CM inserts. It can be equivalent to a very small shunt capacitor across the port and has almost no effect on the antenna. However, in case of the DM, the CPW line is equivalent to a small shunt inductor, greatly influencing the antenna. As shown in Fig. 5, the width of the metal strip *Wm* has more effects on the DM impedance than the CM one. In fact, the metal strip itself also introduces a serial inductor, partly canceling the shunt capacitor of CM and further reducing its effect in CM.

3) Attach a lumped capacitor to connect metal strip and ground plane (antenna IV). The DM impedance has got closer to the matching point after steps 1 and 2. Therefore, all we need to do is to shrink the distance between the CM impedance curve and the DM one. The attached capacitor only affects the CM impedance because the DM virtual PEC boundary will short out it. As shown in Fig. 6, the CM impedance is corresponding to the DM impedance at 1.73 GHz when the lumped capacitor *C* equals to 1.35 pF.

It is noted that some approaches may change the CM/DM impedance simultaneously in reality, which should be brought forward. The whole design steps are generalized in Table II.

D. Design Results

The simulated S-parameters of antennas I–IV are shown in Fig. 7. It can be observed that the antenna achieves better matching performance and higher isolation gradually during the design process. The proposed structure (antenna IV) finally gets isolation maximum of 47.7 dB and good matching at 1.73 GHz.

A comparison of the ideal radiation patterns at 1.73 GHz between the single antenna (a PIFA) and antennas I–IV is given in Fig. 8. The beam direction of the single antenna is toward broadside because it radiates only by one magnetic current. When only port 1 is excited, the beams of antennas I–IV rotate about 20° in E-plane. Take antenna IV as an example. The simulated current complex value distribution at

TABLE I
DESIGN EVOLUTION OF THE PROPOSED ANTENNA

Ant. II	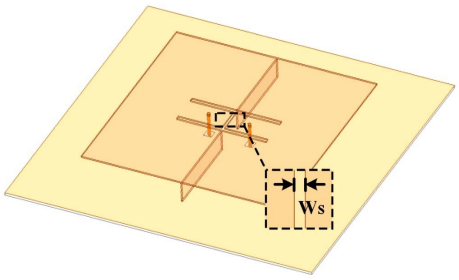
Ant. III	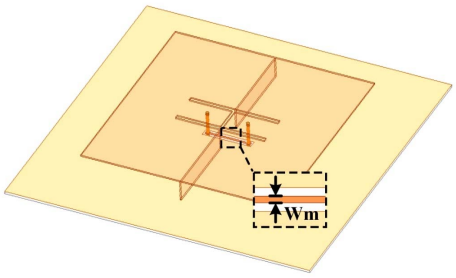
Ant. IV (Proposed)	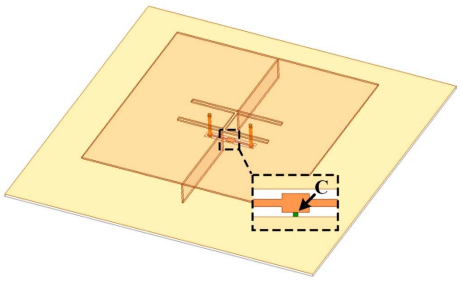

TABLE II
SUMMARY OF DESIGN STEPS

	Step	Function
1	Insert "H" shape slot	Tune both CM and DM impedances
2	Adjust the slot width *Ws*	Tune DM impedance
3	Connect two inner conductors and adjust *Wm*	Tune DM impedance
4	Attach lumped capacitor and adjust *C*	Tune CM impedance

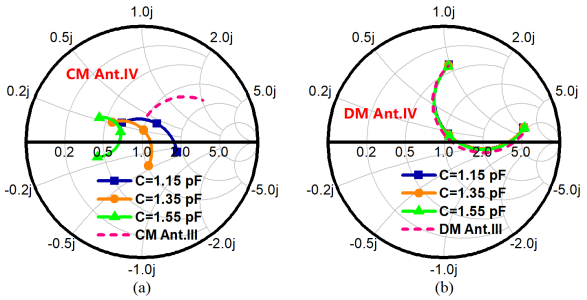

Fig. 6. Impedance smith charts of Antenna IV with varying C. (a) CM. (b) DM.

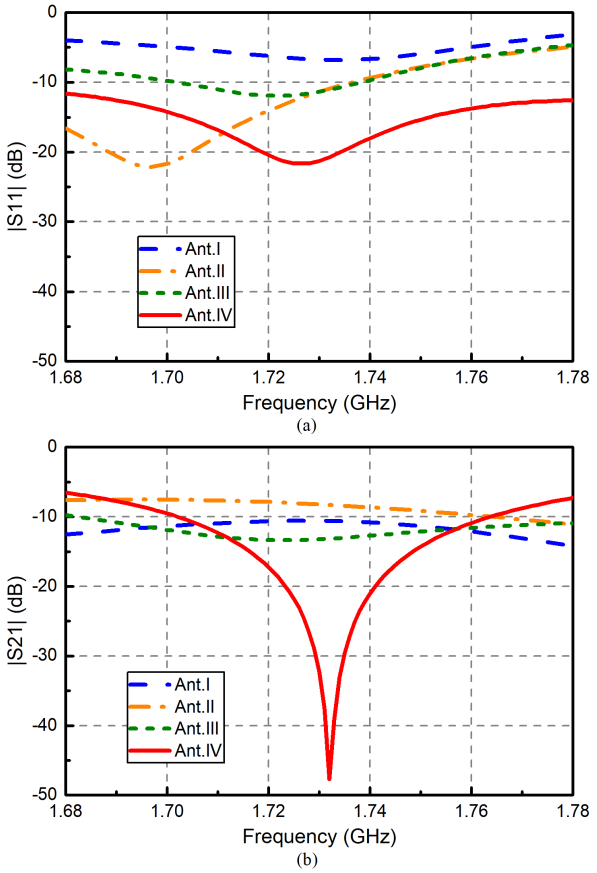

Fig. 7. Simulated S-parameters of Antennas I~IV. (a) Reflection coefficients. (b) Transmission coefficients.

1.73 GHz on the upper board of antenna IV is given in Fig. 9. Although only port 1 is excited, the adjacent element is actually also partly excited at 1.73 GHz. The antenna actually radiates from two magnetic currents. Due to the unequal excitation, the magnitude of the two magnetic currents is different, leading to the beam rotation. Even though the adjacent element is partly excited, port 2 is at the current null point and achieves no power from port 1. It is noted that the simulated cross polarization level of antenna IV in E-plane increases slightly compared with others, but it is still below −30 dB.

III. Antenna Detailed Configuration

The detailed configuration of the proposed antenna is presented in Fig. 10. A 200 mm × 200 mm metal ground plane with a straight slot is printed on one side of a 1 mm-thick

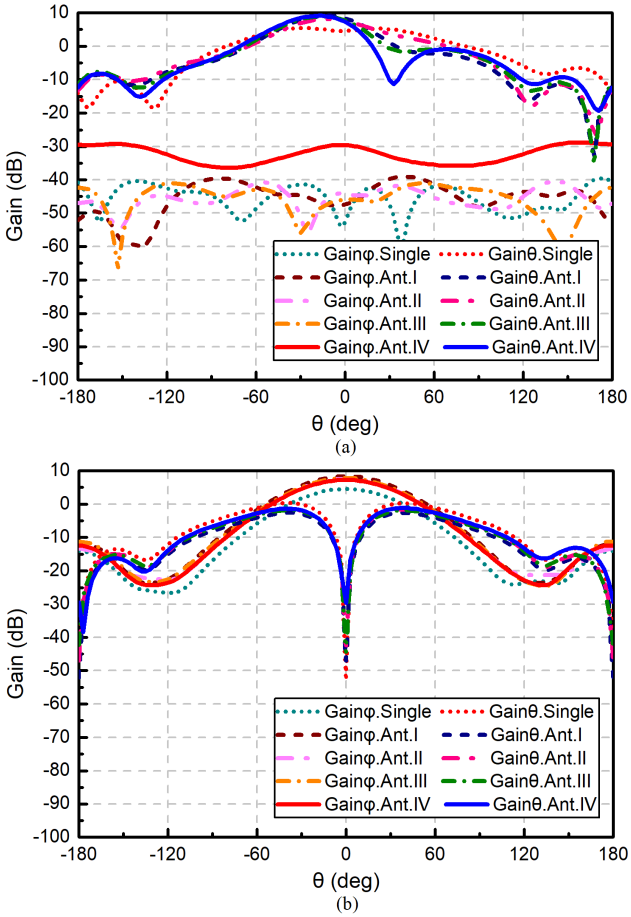

Fig. 8. Simulated gain of a single antenna and antennas I~IV when only port 1 is excited. (a) E-plane. (b) H-plane.

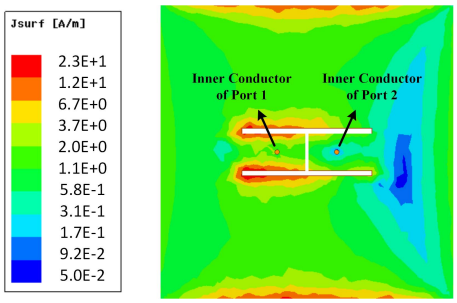

Fig. 9. Simulated current distribution of antenna IV at 1.73 GHz when only port 1 excites.

FR-4 board ($\varepsilon_r = 4.4$, $\tan\delta = 0.02$). Above the ground plane, a 0.5 mm-thick copper board is supported by two vertical 0.5 mm-thick short-circuit walls and 1.2 mm-thick copper cylinders, as shown in Fig. 10(a). An "H"-shaped slot separates the copper board into two PIFAs, which share the same short-circuit walls. The top of the copper cylinder is connected with the copper board, while the end is soldered to the inner conductor of the feeding coaxial cable, as shown in Fig. 10(d). The feeding ports and parts of decoupling structure placed on the other side of the FR-4 board are shown in Fig. 10(c). It is observed that the ground plane has extended to this side by several metal vias and four rectangle panels. Two inner conductors of the feeding coaxial cable are connected by a

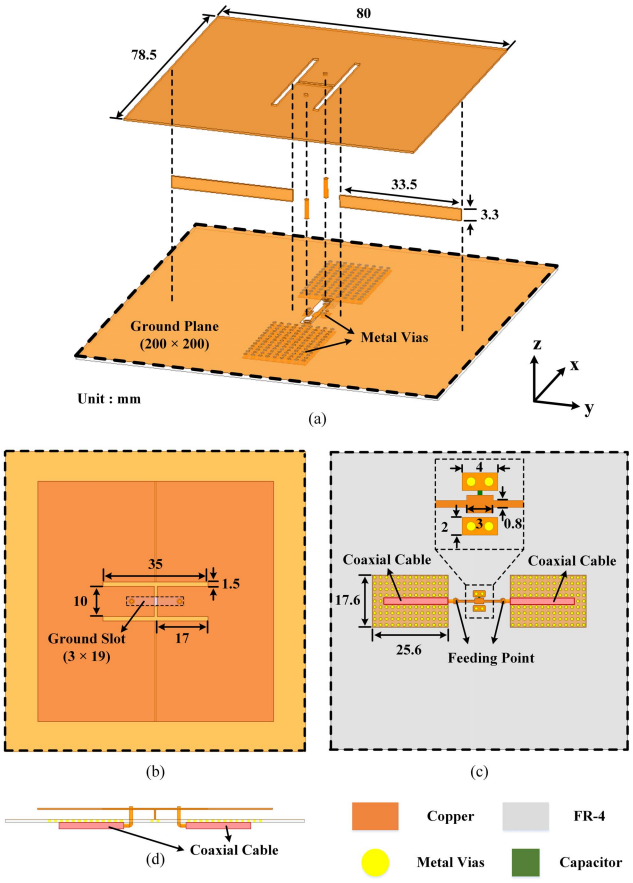

Fig. 10. Detailed geometry of the proposed antenna (nonproportional ground). (a) Exploding view. (b) Top view. (c) Bottom view. (d) Side view.

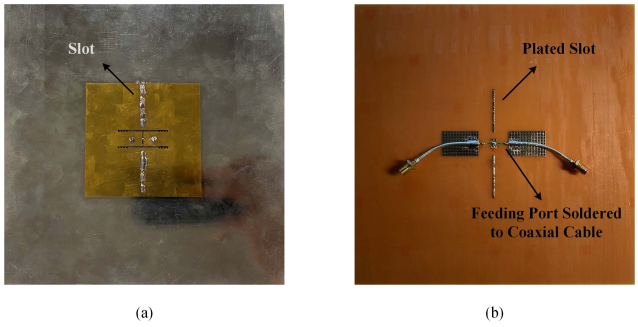

Fig. 11. Photograph of the proposed antenna. (a) Top view. (b) Bottom view.

thin metal strip. A lumped capacitor across the ground panel is attached to the middle of the strip.

IV. Measurement and Discussion

For the purpose of validating the design principle illustrated in Section II, an antenna prototype has been fabricated, as shown in Fig. 11. As is mentioned above, the proposed antenna is with air dielectric. Therefore, additional adjustment is required to support the whole antenna. To this end, the edge shape of two short-circuit walls in Fig. 10(a) is cut into serration. Moreover, several lathy slots are added on both upper copper board and metal ground plane to fit the

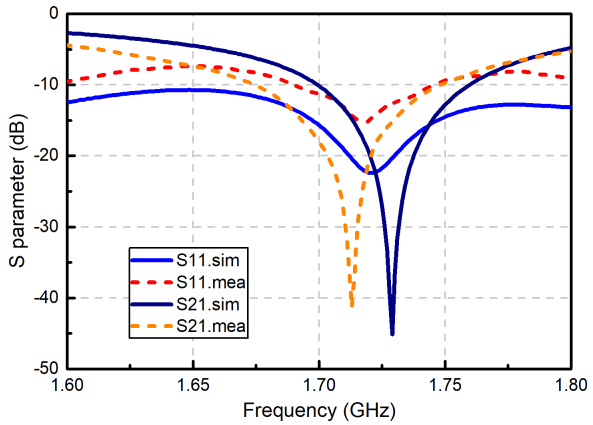

Fig. 12. Simulated and measured S-parameters of the proposed antenna.

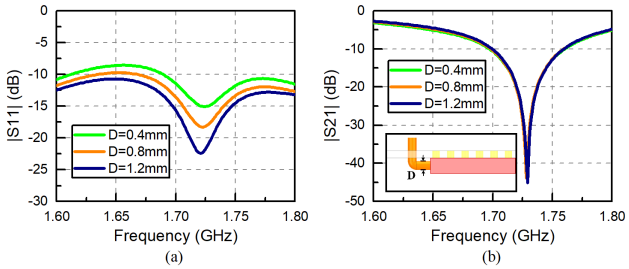

Fig. 13. Simulated S-parameters with varying D. (a) Reflection coefficients. (b) Transmission coefficients.

modified vertical short-circuit walls. Due to these additional adjustments, the final value of the lumped capacitor C is 1.4 pF.

A comparison between the simulated and measured S-parameters is provided in Fig. 12. The measured isolation reaches 42 dB at 1.71 GHz, slightly lower than the simulated result. There is a frequency shift for the decoupling frequency point, mainly because the metal ground plane is uneven. Actually, the unevenness changes the equivalent width and height of the upper copper board. The measured reflection coefficient is below −10 dB from 1.69 to 1.75 GHz, including the decoupling frequency range.

However, the measured reflection coefficients are worse than the simulated ones out of the decoupling frequency range. The reason why measured S_{11} bandwidth gets narrower is illustrated in Fig. 13. The proposed antenna is fed by two coaxial cables. Therefore, a bit of inner conductor will be exposed in the air inevitably, whose diameter is donated as D. This bit of inner conductor is quite thin and introduces an extra serial inductor into the antenna, leading to the deterioration of matching performance. As shown in Fig. 13, the matching performance gets worse with the D decreasing, while the isolation is not affected.

The simulated and measured normalized radiation patterns of the proposed antenna at 1.71 GHz excited from ports 1 and 2 are given in Figs. 14 and 15. The measured results have a good agreement with the simulated ones. The gain maximum points to 20°, with the gain of 1.9 dB higher than broadside. In YOZ plane, the cross polarization level is lower than the co-polarized by 30 dB. It is noted that the proposed antenna is

TABLE III
PERFORMANCES COMPARISON WITH RELEVANT STUDIES

Reference	[3]	[10]	[20]	[28]	This work
Co-polarized Decoupling	No	Yes	Yes	Yes	**Yes**
Substrate Dielectric Constant	10	2.2	1*	3.55	**1***
Size	$0.2\lambda_0\times0.38\lambda_0$	$1.9\lambda_0\times1.9\lambda_0$	$1.68\lambda_0\times0.64\lambda_0$	$0.86\lambda_0\times0.58\lambda_0$	**$0.45\lambda_0\times0.45\lambda_0$**
Edge-to-Edge Distance	$0.033\lambda_0$	NA	$0.92\lambda_0$	$0.03\lambda_0$	**0**
Profile	$0.017\lambda_0$	$0.016\lambda_0$	$0.013\lambda_0$	$0.25\lambda_0$	**$0.02\lambda_0$**
Isolation Maximum	50 dB	50 dB	80 dB	50 dB	**42 dB**
>20dB Isolation Bandwidth	1.2%	16.7%	11%	1.4%	**1.2%**
Efficiency	78.5%	80%	94%	NA	**90%**

*Adopt air dielectric and use FR-4 as upholder.

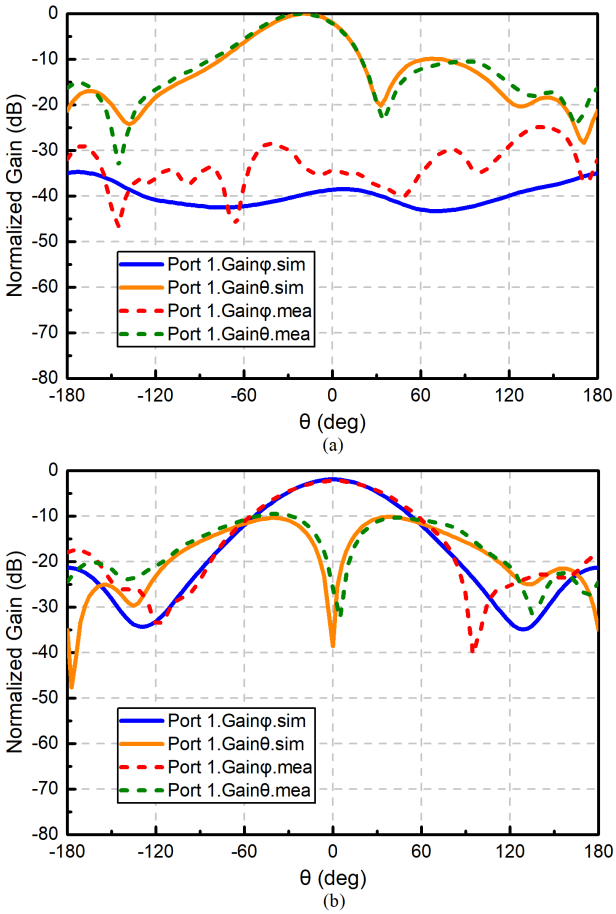

Fig. 14. Simulated and measured normalized pattern at 1.71 GHz when only port 1 is excited. (a) YOZ plane. (b) XOZ plane.

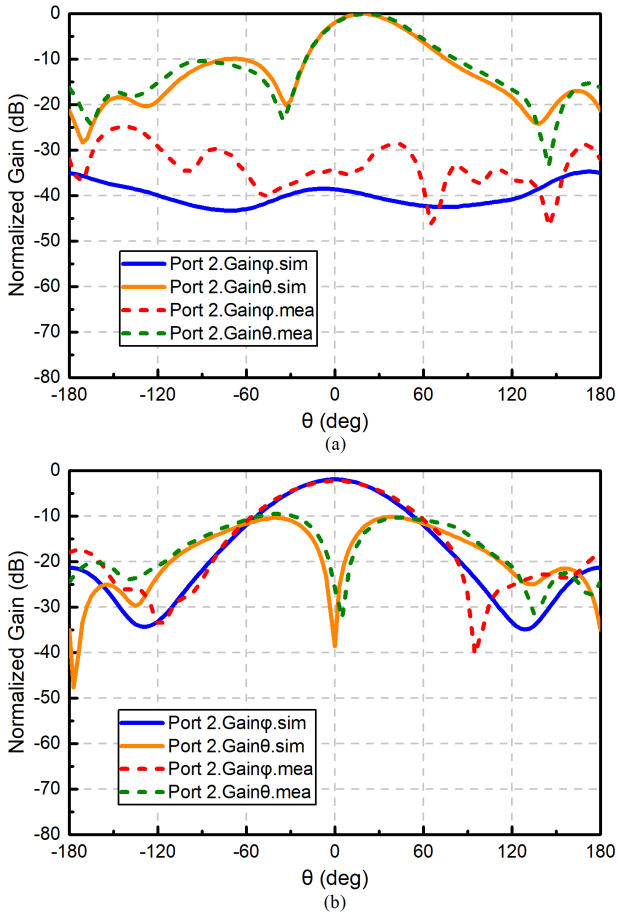

Fig. 15. Simulated and measured normalized pattern at 1.71 GHz when only port 2 is excited. (a) YOZ plane. (b) XOZ plane.

symmetric about XOZ and YOZ plane. Therefore, the radiation patterns are symmetrical in E-plane and same in H-plane when it is fed by ports 1 and 2, respectively.

Fig. 16 shows the in-band gain curves and total efficiency of the proposed antenna, where the gray region represents the range of measured isolation higher than 20 dB. The measured gain maximum is 8.6 dBi, slightly lower than the simulated gain of 9 dBi. The gain difference at higher frequency mainly comes from the impedance matching deterioration caused by exposed coaxial cable inner conductors. The proposed antenna achieves high measured efficiency of 90% in the working band, owing to its air dielectric structure. The FR-4 board is used

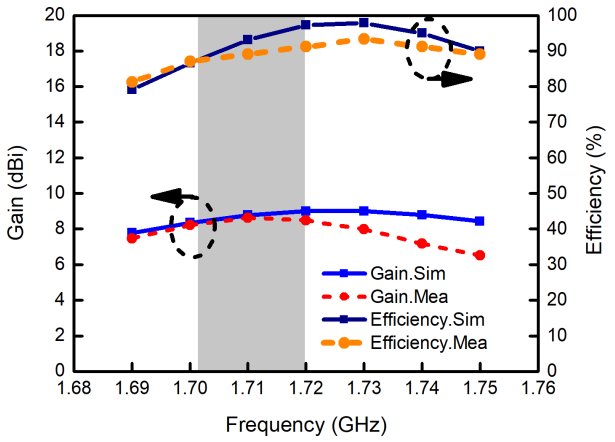

Fig. 16. Simulated and measured normalized pattern in XOZ plane.

to support the metal ground plane and has few influences on the antenna efficiency.

A comprehensive comparison between the proposed antenna and other relevant researches is listed in Table III. The isolation maximums of all works are higher than 40 dB. It can be observed that the proposed antenna has the smallest edge-to-edge distance and electrical size among all co-polarized full-duplex works.

V. Conclusion

In this work, a compact co-polarized low-profile antenna for full-duplex application at 1.71 GHz is proposed. There is no edge-to-edge distance between the two air-dielectric PIFA units. The antenna is designed and analyzed based on the CM/DM cancellation theory. The measured mutual coupling reduction reaches 42 dB and the measured efficiency of 90% is achieved. The gain maximum of the proposed antenna is up to 8.6 dBi, with a little gain variation of 1.9 dB when comes to the broadside.

References

[1] D. Wojcik, M. Surma, A. Noga, and M. Magnuski, "High port-to-port isolation dual-polarized antenna array dedicated for full-duplex base stations," *IEEE Antennas Wireless Propag. Lett.*, vol. 19, no. 7, pp. 1098–1102, Jul. 2020.

[2] X. Wang, W. Che, W. Yang, W. Feng, and L. Gu, "Self-interference cancellation antenna using auxiliary port reflection for full-duplex application," *IEEE Antennas Wireless Propag. Lett.*, vol. 16, pp. 2873–2876, 2017.

[3] K. Wei and B.-C. Zhu, "The novel w parasitic strip for the circularly polarized microstrip antennas design and the mutual coupling reduction between them," *IEEE Trans. Antennas Propag.*, vol. 67, no. 2, pp. 804–813, Feb. 2019.

[4] B. Feng, L. Li, J.-C. Cheng, and C.-Y.-D. Sim, "A dual-band dual-polarized stacked microstrip antenna with high-isolation and band-notch characteristics for 5G microcell communications," *IEEE Trans. Antennas Propag.*, vol. 67, no. 7, pp. 4506–4516, Jul. 2019.

[5] Y. He and Y. Li, "Dual-polarized microstrip antennas with capacitive via fence for wide beamwidth and high isolation," *IEEE Trans. Antennas Propag.*, vol. 68, no. 7, pp. 5095–5103, Jul. 2020.

[6] Y. Cui, Y. Niu, Y. Qin, and R. Li, "A new high-isolation broadband flush-mountable dual-polarized antenna," *IEEE Trans. Antennas Propag.*, vol. 66, no. 12, pp. 7342–7347, Dec. 2018.

[7] O. N. Alrabadi, A. D. Tatomirescu, M. B. Knudsen, M. Pelosi, and G. F. Pedersen, "Breaking the transmitter–receiver isolation barrier in mobile handsets with spatial duplexing," *IEEE Trans. Antennas Propag.*, vol. 61, no. 4, pp. 2241–2251, Apr. 2013.

[8] D. Wu, Y.-X. Sun, B. Wang, and R. Lian, "A compact, monostatic, co-circularly polarized simultaneous transmit and receive (STAR) antenna with high isolation," *IEEE Antennas Wireless Propag. Lett.*, vol. 19, no. 7, pp. 1127–1131, Jul. 2020.

[9] L. Sun, Y. Li, Z. Zhang, and Z. Feng, "Compact co-horizontally polarized full-duplex antenna with omnidirectional patterns," *IEEE Antennas Wireless Propag. Lett.*, vol. 18, no. 6, pp. 1154–1158, Jun. 2019.

[10] Z. Zhou, Y. Li, J. Hu, Y. He, Z. Zhang, and P.-Y. Chen, "Monostatic copolarized simultaneous transmit and receive (STAR) antenna by integrated single-layer design," *IEEE Antennas Wireless Propag. Lett.*, vol. 18, no. 3, pp. 472–476, Mar. 2019.

[11] J. Wu, M. Li, and N. Behdad, "A wideband, unidirectional circularly polarized antenna for full-duplex applications," *IEEE Trans. Antennas Propag.*, vol. 66, no. 3, pp. 1559–1563, Mar. 2018.

[12] J. Ha, M. A. Elmansouri, P. V. Prasannakumar, and D. S. Filipovic, "Monostatic co-polarized full-duplex antenna with left-or right-hand circular polarization," *IEEE Trans. Antennas Propag.*, vol. 65, no. 10, pp. 5103–5111, Oct. 2017.

[13] M. A. Elmansouri, A. J. Kee, and D. S. Filipovic, "Wideband antenna array for simultaneous transmit and receive (STAR) applications," *IEEE Antennas Wireless Propag. Lett.*, vol. 16, pp. 1277–1280, 2017.

[14] W.-G. Lim, W.-I. Son, K. S. Oh, W.-K. Kim, and J.-W. Yu, "Compact integrated antenna with circulator for UHF RFID system," *IEEE Antennas Wireless Propag. Lett.*, vol. 7, pp. 673–675, 2008.

[15] E. A. Etellisi, M. A. Elmansouri, and D. S. Filipovic, "Wideband monostatic simultaneous transmit and receive (STAR) antenna," *IEEE Trans. Antennas Propag.*, vol. 64, no. 1, pp. 6–15, Jan. 2016.

[16] E. A. Etellisi, M. A. Elmansouri, and D. S. Filipovic, "In-band full-duplex multimode lens-loaded eight-arm spiral antenna," *IEEE Trans. Antennas Propag.*, vol. 66, no. 4, pp. 2084–2089, Apr. 2018.

[17] R. Lian, T.-Y. Shih, Y. Yin, and N. Behdad, "A high-isolation, ultra-wideband simultaneous transmit and receive antenna with monopole-like radiation characteristics," *IEEE Trans. Antennas Propag.*, vol. 66, no. 2, pp. 1002–1007, Feb. 2018.

[18] E. A. Etellisi, M. A. Elmansouri, and D. S. Filipovic, "Wideband monostatic co-polarized co-channel simultaneous transmit and receive broadside circular array antenna," *IEEE Trans. Antennas Propag.*, vol. 67, no. 2, pp. 843–852, Feb. 2019.

[19] J.-H. Xun, L.-F. Shi, W.-R. Liu, and D.-J. Xin, "A self-interference suppression structure for collinear dipoles," *IEEE Antennas Wireless Propag. Lett.*, vol. 18, no. 10, pp. 2100–2104, Oct. 2019.

[20] K. Iwamoto, M. Heino, K. Haneda, and H. Morikawa, "Design of an antenna decoupling structure for an inband full-duplex collinear dipole array," *IEEE Trans. Antennas Propag.*, vol. 66, no. 7, pp. 3763–3768, Jul. 2018.

[21] B. K. Lau and J. B. Andersen, "Simple and efficient decoupling of compact arrays with parasitic scatterers," *IEEE Trans. Antennas Propag.*, vol. 60, no. 2, pp. 464–472, Feb. 2012.

[22] K. S. Vishvaksenan, K. Mithra, R. Kalaiarasan, and K. S. Raj, "Mutual coupling reduction in microstrip patch antenna arrays using parallel coupled-line resonators," *IEEE Antennas Wireless Propag. Lett.*, vol. 16, pp. 2146–2149, 2017.

[23] A. Kord, D. L. Sounas, and A. Alu, "Magnet-less circulators based on spatiotemporal modulation of bandstop filters in a delta topology," *IEEE Trans. Microw. Theory Techn.*, vol. 66, no. 2, pp. 911–926, Feb. 2018.

[24] X.-L. Li, G.-M. Yang, and Y.-Q. Jin, "Isolation enhancement of wideband vehicular antenna array using fractal decoupling structure," *IEEE Antennas Wireless Propag. Lett.*, vol. 18, no. 9, pp. 1799–1803, Sep. 2019.

[25] M. Niroo-Jazi, T. A. Denidni, M. R. Chaharmir, and A. R. Sebak, "A hybrid isolator to reduce electromagnetic interactions between Tx/Rx antennas," *IEEE Antennas Wireless Propag. Lett.*, vol. 13, pp. 75–78, 2014.

[26] H. S. Farahani, M. Veysi, M. Kamyab, and A. Tadjalli, "Mutual coupling reduction in patch antenna arrays using a UC-EBG superstrate," *IEEE Antennas Wireless Propag. Lett.*, vol. 9, pp. 57–59, 2010.

[27] E. Rajo-Iglesias, Ó. Quevedo-Teruel, and L. Inclan-Sanchez, "Mutual coupling reduction in patch antenna arrays by using a planar EBG structure and a multilayer dielectric substrate," *IEEE Trans. Antennas Propag.*, vol. 56, no. 6, pp. 1648–1655, Jun. 2008.

[28] H. Qi, L. Liu, X. Yin, H. Zhao, and W. J. Kulesza, "Mutual coupling suppression between two closely spaced microstrip antennas with an asymmetrical coplanar strip wall," *IEEE Antennas Wireless Propag. Lett.*, vol. 15, pp. 191–194, 2016.

[29] M.-C. Tang *et al.*, "Mutual coupling reduction using meta-structures for wideband, dual-polarized, and high-density patch arrays," *IEEE Trans. Antennas Propag.*, vol. 65, no. 8, pp. 3986–3998, May 2017.
[30] Y.-F. Cheng, X. Ding, W. Shao, and B.-Z. Wang, "Reduction of mutual coupling between patch antennas using a polarization-conversion isolator," *IEEE Antennas Wireless Propag. Lett.*, vol. 16, pp. 1257–1260, 2017.
[31] H. Li, B. K. Lau, and S. He, "Design of closely packed pattern reconfigurable antenna array for MIMO terminals," *IEEE Trans. Antennas Propag.*, vol. 65, no. 9, pp. 4891–4896, Sep. 2017.
[32] A. Habashi, J. Nourinia, and C. Ghobadi, "Mutual coupling reduction between very closely spaced patch antennas using low-profile folded split-ring resonators (FSRRs)," *IEEE Antennas Wireless Propag. Lett.*, vol. 10, pp. 862–865, 2011.
[33] S. Zhang, B. K. Lau, Y. Tan, Z. Ying, and S. He, "Mutual coupling reduction of two PIFAs with a T-shape slot impedance transformer for MIMO mobile terminals," *IEEE Trans. Antennas Propag.*, vol. 60, no. 3, pp. 1521–1531, Mar. 2012.
[34] S.-H. Zhu, X.-S. Yang, J. Wang, and B.-Z. Wang, "Design of MIMO antenna isolation structure based on a hybrid topology optimization method," *IEEE Trans. Antennas Propag.*, vol. 67, no. 10, pp. 6298–6307, Oct. 2019.
[35] E. A. Etellisi, M. A. Elmansouri, and D. S. Filipovic, "Wideband multimode monostatic spiral antenna STAR subsystem," *IEEE Trans. Antennas Propag.*, vol. 65, no. 4, pp. 1845–1854, Apr. 2017.
[36] M. R. Nikkhah, J. Wu, H. Luyen, and N. Behdad, "A concurrently dual-polarized, simultaneous transmit and receive (STAR) antenna," *IEEE Trans. Antennas Propag.*, vol. 68, no. 8, pp. 5935–5944, Aug. 2020.
[37] C. Lu, Q. Zhang, H. Qi, S. Li, H. Zhao, and X. Yin, "Compact postwall slotline-based stepped impedance resonator decoupling structure for isolation enhancement of patch antenna array," *IEEE Antennas Wireless Propag. Lett.*, vol. 18, no. 12, pp. 2647–2651, Dec. 2019.
[38] L. Sun, Y. Li, Z. Zhang, and H. Wang, "Antenna decoupling by common and differential modes cancellation," *IEEE Trans. Antennas Propag.*, vol. 69, no. 2, pp. 672–682, Feb. 2021.
[39] L. Sun, Y. Li, and Z. Zhang, "Decoupling between extremely closely-spaced patch antennas by mode cancellation method," *IEEE Trans. Antennas Propag.*, early access, Oct. 20, 2020, doi: 10.1109/TAP.2020.3030922.
[40] H. Xu, S. S. Gao, H. Zhou, H. Wang, and Y. Cheng, "A highly integrated MIMO antenna unit: Differential/common mode design," *IEEE Trans. Antennas Propag.*, vol. 67, no. 11, pp. 6724–6734, Nov. 2019.
[41] D. E. Bockelman and W. R. Eisenstadt, "Combined differential and common-mode scattering parameters: Theory and simulation," *IEEE Trans. Microw. Theory Techn.*, vol. 43, no. 7, pp. 1530–1539, Jul. 1995.
[42] J.-S. Hong, *Microstrip Filters for RF/Microwave Applications*. Hoboken, NJ, USA: Wiley, 2010.

Jiadong Hu received the B.S. degree from Xidian University, Xi'an, China, in 2017. He is currently pursuing the Ph.D. degree in electrical engineering with Tsinghua University, Beijing, China.

His current research interests include antenna decoupling, reconfigurable antennas, and beam scanning array.

Weiquan Zhang received the B.S. degree from the University of Electronic Science and Technology of China, Chengdu, China, in 2018. He is currently pursuing the Ph.D. degree in electrical engineering with Tsinghua University, Beijing, China.

His current research interests include reconfigurable antennas, multimode antennas, and reflectarray antennas.

Yue Li (Senior Member, IEEE) received the B.S. degree in telecommunication engineering from Zhejiang University, Zhejiang, China, in 2007, and the Ph.D. degree in electronic engineering from Tsinghua University, Beijing, China, in 2012.

He is currently an Associate Professor with the Department of Electronic Engineering, Tsinghua University. In June 2012, he was a Post-Doctoral Fellow with the Department of Electronic Engineering, Tsinghua University. In December 2013, he was a Research Scholar with the Department of Electrical and Systems Engineering, University of Pennsylvania, Philadelphia, PA, USA. He was also a Visiting Scholar with the Institute for Infocomm Research (I2R), A∗STAR, Singapore, in 2010, and the Hawaii Center of Advanced Communication (HCAC), University of Hawaii at Manoa, Honolulu, HI, USA, in 2012. Since January 2016, he has been with Tsinghua University, where he is an Assistant Professor. He has authored or coauthored over 150 journal papers and 45 international conference papers, and holds 20 granted Chinese patents. His current research interests include metamaterials, plasmonics, electromagnetics, nanocircuits, mobile and handset antennas, MIMO and diversity antennas, and millimeter-wave antennas and arrays.

Dr. Li was a recipient of the Issac Koga Gold Medal from the URSI General Assembly in 2017; the Second Prize of Science and Technology Award of the China Institute of Communications in 2017; the Young Scientist Awards from the conferences of PIERS 2019, ACES 2018, AT-RASC 2018, AP-RASC 2016, EMTS 2016, and URSI GASS 2014; the Best Paper Awards from the conferences of APCAP 2020/2017, UCMMT 2020, ISAP 2019, CSQRWC 2018, NCMMW 2018/2017, NCANT 2019/2017, ISAPE 2016, and ICMMT 2020/2016; the Outstanding Doctoral Dissertation of Beijing Municipality in 2013; and the Principal Scholarship of Tsinghua University in 2011. He serves an Associate Editor for the IEEE TRANSACTIONS ON ANTENNAS AND PROPAGATION, the IEEE ANTENNAS AND WIRELESS PROPAGATION LETTERS, *Microwave and Optical Technology Letters*, and *Computer Applications in Engineering Education*, and also as an Editorial Board Member of *Scientific Report*.

Zhijun Zhang (Fellow, IEEE) received the B.S. and M.S. degrees from the University of Electronic Science and Technology of China, Chengdu, China, in 1992 and 1995, respectively, and the Ph.D. degree from Tsinghua University, Beijing, China, in 1999.

In 1999, he was a Post-Doctoral Fellow with the Department of Electrical Engineering, The University of Utah, Salt Lake City, UT, USA, where he was appointed a Research Assistant Professor in 2001. In May 2002, he was an Assistant Researcher with the University of Hawaii at Manoa, Honolulu, HI, USA. In November 2002, he joined Amphenol T&M Antennas, Vernon Hills, IL, USA, as a Senior Staff Antenna Development Engineer and was then promoted to the position of Antenna Engineer Manager. In 2004, he joined Nokia Inc., San Diego, CA, USA, as a Senior Antenna Design Engineer. In 2006, he joined Apple Inc., Cupertino, CA, as a Senior Antenna Design Engineer and was then promoted to the position of Principal Antenna Engineer. Since August 2007, he has been with Tsinghua University, where he is a Professor with the Department of Electronic Engineering. He is the author of *Antenna Design for Mobile Devices* (Wiley, First Edition 2011, Second Edition 2017).

Dr. Zhang served as an Associate Editor for the IEEE TRANSACTIONS ON ANTENNAS AND PROPAGATION from 2010 to 2014 and the IEEE ANTENNAS AND WIRELESS PROPAGATION LETTERS from 2009 to 2015.